

1 **PALeo constraints on SEA level rise (PALSEA): ice-sheet and sea-level responses to**  
2 **past climate warming**

3 Anders E. Carlson <sup>a,\*</sup>, Andrea Dutton <sup>b</sup>, Antony J. Long <sup>c</sup>, Glenn A. Milne <sup>d</sup>

4 <sup>a</sup> *College of Earth, Ocean, and Atmospheric Sciences, Oregon State University, Corvallis, OR,*  
5 *USA 97331*

6 <sup>b</sup> *Department of Geological Sciences, University of Florida, Gainesville, FL, USA 32611*

7 <sup>c</sup> *Department of Geography, Durham University, Durham DH1 3LE, UK*

8 <sup>d</sup> *Department of Earth and Environmental Sciences, University of Ottawa, ON, K1N 6N5,*  
9 *Canada*

10 [\\*acarlson@coas.oregonstate.edu](mailto:acarlson@coas.oregonstate.edu)

11 **ABSTRACT**

12 Here we summarize the motivation and issues surrounding the responses of ice sheets and sea  
13 level to past climate warming as part of the PALeo constraints on SEA level rise (PALSEA)  
14 working group. Papers in this special issue of *Quaternary Science Reviews* focus on the timescale  
15 of glaciations during the late Pliocene, the magnitude of ice-sheet fluctuations and volume leading  
16 up to and during the last glacial maximum, the timing and persistence of ice-sheet impacts on  
17 deglacial and future relative sea-level change, and relative sea-level change during peak  
18 interglacial climate. A more dynamic cryosphere is noted under both late Pliocene and last glacial  
19 cycle climate conditions, while relative sea-level changes during the last deglaciation appear to  
20 correspond closely with individual ice-sheet deglaciation. Lastly, relative sea-level change during  
21 peak interglacial conditions may have fluctuated by as much as a meter, although the sources of  
22 such variability (Greenland, Antarctica or elsewhere) remain elusive.

23 **1. Introduction**

24 The greatest uncertainty in projecting future sea-level rise lies in the responses of Earth's  
25 remaining ice sheets (e.g., Alley et al., 2005; Church et al., 2013; Clark et al., 2016). The

26 observational period of sea level and ice-sheet mass balance spans at best only the last century,  
27 at least partly exacerbating present uncertainty in future sea-level rise (Church et al., 2013). In  
28 contrast, the geologic record provides valuable archives of how ice sheets and sea level have  
29 responded to past climate variability, particularly during periods of climate warming (e.g., Alley et  
30 al., 2005; Dutton et al., 2015a; Clark et al., 2016). The information contained in the geological  
31 record can therefore help assess the relationship between ice sheets, sea level and climate  
32 change over multi-millennial to century timescales.

33 PALeo constraints on SEA level rise 2 (PALSEA2) is a Past Global Changes (PAGES)  
34 working group and international focus group of the Coastal and Marine Processes commission in  
35 International Union for Quaternary Research (INQUA). PALSEA brings together observational  
36 scientists and ice-sheet, climate and sea-level modelers in order to better define and interpret  
37 observational constraints on past sea-level rise and improve our understanding of ice-sheet  
38 responses to climate change. This PALSEA *Quaternary Science Reviews* special issue  
39 addresses these topics by examining orbital-scale sea-level changes during the late Pliocene  
40 (Grant et al., 2018), ice-sheet extent and volume prior to and during the last glacial maximum  
41 (Carlson et al., 2018; Pico et al., 2018; Simms et al., 2019), relative sea-level changes following  
42 the last glacial maximum (Barnett et al., 2019; Romundset et al., 2018; Simms et al., 2018; Xiong  
43 et al., 2018; Yokoyama et al., 2019; Yousefi et al., 2018), and full interglacial relative sea-level  
44 change during the last interglaciation (Skrivanek et al., 2018) (Fig. 1, 2b). Here we summarize  
45 and contextualize the findings of these studies and lay a road map for future research on past ice-  
46 sheet and sea-level change.

## 47 **2. Sea level variability in warm times**

48 The late Pliocene of 3,300 to 3,000 ka (Fig. 2b) is the last time that atmospheric CO<sub>2</sub>  
49 concentrations were around present-day values (Fig. 2c), providing an important long-term  
50 constraint on the response of the cryosphere to this radiative forcing (Alley et al., 2005; Dutton et

51 al., 2015a). However, geophysical processes such as mantle dynamic topography have likely  
52 caused sea-level indicators to change in elevation since the time of their formation. This  
53 complicates the procedure to estimate global-mean sea level from these records (e.g., Dutton et  
54 al., 2015a). However, orbital-scale fluctuations in temperature and ice volume certainly occurred  
55 across this 300-ka time window followed by the descent of the Earth into the Pleistocene ice ages  
56 (Fig. 2a, b).

57 Grant et al. (2018) provide a new insight into late-Pliocene changes in relative sea level in the  
58 Whanganui Basin, New Zealand (1 on Fig. 1). Here, a marginal marine basin records 23  
59 sedimentary cycles related to the rise and fall of local sea level from 3,300 to 2,600 ka, which are  
60 dated by magnetostratigraphy, biostratigraphy and tephra chronology that are largely  
61 independent of orbital tuning. Interestingly, sea level fluctuated at a 20-ka timescale 3,300 to  
62 3,000 ka, then switched to a 40-ka timescale 3,000 to 2,600 ka; these periodicities are reminiscent  
63 of, respectively, precession and obliquity timescales of Quaternary ice-sheet fluctuations. Grant  
64 et al. (2018) note that they can find a one-to-one correlation between their sea-level changes and  
65 a high-resolution benthic  $\delta^{18}\text{O}$  record from the eastern tropical Pacific (Mix et al., 1995), which is  
66 not found in the benthic  $\delta^{18}\text{O}$  stack in Fig. 2b (Lisiecki & Raymo, 2005). Spectral power at the  
67 precession frequency is largely lacking in the benthic  $\delta^{18}\text{O}$  stack across the late Pliocene to early  
68 Quaternary when that due to obliquity is dominant (Raymo et al., 2006; Meyers & Hinnov, 2010).  
69 Grant et al. (2018) suggest that this mismatch could be due to smoothing of the benthic  $\delta^{18}\text{O}$   
70 records in the stacking process or the low resolution of some of the contributing records.

### 71 **3. The last glacial cycle**

72 Individual ice-sheet sources of sea-level change prior to the last glacial maximum are difficult  
73 to interpret because the terrestrial record of ice-sheet extent (and inferred volume) is largely  
74 removed by the ice sheets during the last glacial maximum (e.g., Clark et al., 1993; Dyke et al.,  
75 2002) and far-field sea level indicators may not have a unique solution for individual ice-sheet

76 sources (e.g., Peltier & Fairbanks, 2006; Lambeck et al., 2014). However, Pico et al. (2017) were  
77 able to use relative sea-level indicators along the eastern seaboard of the United States to  
78 document a smaller Laurentide ice-sheet volume during marine isotope stage (MIS) 3, 60-26 ka  
79 (2,3 on Fig. 2b), than is used in current sea level-ice volume solutions (e.g., Peltier & Fairbanks,  
80 2006; Lambeck et al., 2014). Relatively unique geological constraints are preserved in the Hudson  
81 Bay lowlands that indicate ice-free conditions in the center of the Laurentide ice sheet for the first  
82 half of MIS 3 (Fig. 1) (Dalton et al., 2016; 2019). Pico et al. (2018) present a revised ice model  
83 from the 2017 study (3 on Fig. 1), which better agrees with the geological constraints. Carlson et  
84 al. (2018) also addressed MIS 3 Laurentide ice-extent changes, documenting a late MIS 3  
85 advance to near the last glacial maximum extent of the Laurentide ice sheet by ~39 ka (2 on Fig.  
86 1). The timing of this MIS 3 maximum is in agreement with other Laurentide ice-margin constraints  
87 (Wood et al., 2011; Ceperley et al., 2019 in press) and requires rapid growth of the Laurentide ice  
88 sheet. In this vein, Carlson et al. (2018) and Pico et al. (2018) use independent dynamic ice-sheet  
89 simulations to show that rapid advance is glaciologically possible, and was the case leading into  
90 the last glacial maximum.

91 While not a warming climate, the last glacial maximum does set the stage for the last period  
92 of global warming (the last deglaciation) prior to that of the last century. However, the sources of  
93 the sea-level lowering during the last glacial maximum has been debated since the first  
94 chronological constraints showed that most Quaternary ice sheets were concurrently at their last  
95 glacial maximum extent (Donn et al., 1962; Denton & Hughes, 1981; Clark & Mix, 2002; Clark et  
96 al., 2009; Clark & Tarasov, 2014). Specifically, individual ice-sheet volumes do not sum up to the  
97 estimated eustatic sea-level lowering at the last glacial maximum (4 on Fig. 2b). Simms et al.  
98 (2019) revisit this plaguing issue by looking for additional sources of sea-level lowering beyond  
99 global ice sheets (4 on Fig. 1). They estimate a low-stand contribution from ocean steric  
100 contraction of ~2.4 m and groundwater storage of ~1.4 m. While these contributions help to push

101 the budget towards balance, there still remains a considerable deficit, implying error in either the  
102 ice-sheet reconstructions or the volume estimated from far-field sea-level records.

103 For the last deglaciation, four studies focus on relative sea-level changes from near,  
104 intermediate, and far-field locations (numbers 5-8 on Fig. 1). Yousefi et al. (2018) assess the  
105 glacial isostatic adjustment (GIA) in sea-level indicators along the western Northern American  
106 coast from southern Canada to the southern United States. They found significant mantle  
107 viscosity variability across this tectonically active region. They demonstrate that GIA can  
108 contribute up to ~20 cm in sea-level rise along this coast by 2100 C.E. and so should be included  
109 in future projections for this region. Their results also indicate that all of the glaciological  
110 reconstructions considered (~25 in total) include the onset of major deglaciation that is too early  
111 to be consistent with the deglacial relative sea-level indicators. This is important as new <sup>10</sup>Be  
112 surface exposure ages for this region indicate initial coast deglaciation at ~17 ka, even earlier  
113 than in the ice-sheet loading histories (Darvill et al., 2018; Lesnek et al., 2018). Rectifying these  
114 apparently disparate observations would require relatively minimal and localized ice-margin  
115 retreat at ~17 ka, followed several millennia later by more significant retreat and deglaciation, with  
116 implications for the timing of when an ice-free coast could form along western North America for  
117 human migration southwards into the contiguous United States.

118 Romundset et al. (2018) present a new near-field relative sea-level record for southeastern  
119 Norway (6 on Fig. 1) at century-scale resolution. A major inflection in relative sea-level fall at ~9.5  
120 ka shows excellent agreement with the timing of full Scandinavian ice sheet deglaciation dated  
121 by <sup>10</sup>Be surface exposure ages (Cuzzone et al., 2016). Later variations in the rate of sea-level fall  
122 (e.g., event around 7 ka) likely reflect sea-surface height signals from distant ice sheets. The  
123 relative sea-level data resulting from this study will provide important constraints on GIA models  
124 and therefore for improving predictions of future sea-level change in this region.

125 Xiong et al. (2018) and Yokoyama et al. (2019) (7 and 8, respectively, on Fig. 1) update far-  
126 field relative sea-level records from the South China Sea and northern Indian Ocean, respectively.  
127 Xiong et al. (2018) note an acceleration in relative sea-level rise at ~9.5 ka with a slowing sea-  
128 level rise at ~7.0 ka. These are times of known acceleration in Laurentide ice sheet retreat and  
129 final deglaciation (Carlson et al., 2008a; Ullman et al., 2016). Yokoyama et al. (2019) document  
130 the timing of cessation in global mean sea-level rise to be ~4 ka, placing an important constraint  
131 on global ice volume change following this time. These findings agree with prior far-field  
132 assessments (Hallmann et al., 2018) and inferences from individual ice-sheet records (Cuzzone  
133 et al., 2016; Ullman et al., 2016). These findings would also place the end of the last deglaciation  
134 at ~4 ka, meaning true peak interglacial conditions, as defined by a maximum in global mean sea  
135 level, only occurred during approximately the last 1/3 of the Holocene.

#### 136 **4. Interglacial relative sea-level change**

137 The last interglaciation (128-116 ka) is three times as long as the Holocene interglaciation  
138 (4.0-0 ka) (Dutton et al., 2015b; Barlow et al., 2018; Polyak et al., 2018; Yokoyama et al., 2019),  
139 if defined by global mean sea level at or above pre-industrial levels (Fig. 2b). Although global  
140 mean sea-level change of the last 4 ka has been on the centimeter to decimeter scale (e.g., Kopp  
141 et al., 2016), last interglacial sea level may have fluctuated on a meter scale (e.g., Kopp et al.,  
142 2013). Given the implications for ice-volume changes, a major question then is determining the  
143 time period over which such a fluctuation occurred. Helping in solving this question, Skrivanek et  
144 al. (2018) revisit coral elevations and stratigraphy on the Bahamas (9 on Fig. 1) where such a  
145 sea-level oscillation was previously suggested (Thompson et al., 2011). Skrivanek et al. (2018)  
146 confirm a transient relative sea-level fall and rise of at least 1 m in ~1 ka. This finding does not  
147 necessarily conflict with a new sea-level record from the Mediterranean that could rule out a larger  
148 sea-level oscillation of >1 m in magnitude at that location (Polyak et al., 2018). The cause of this  
149 oscillation at the Bahamas is, however, unknown (Barlow et al., 2018).

150 Simms et al. (2018) and Barnett et al. (2018) provide two new relative sea-level records to  
151 document peak interglacial Holocene change at near-field sites on the Antarctic Peninsula (10 on  
152 Fig. 1) and eastern Quebec (11 on Fig. 1), respectively. Simms et al. (2018) find changes in sea  
153 level along the Antarctic Peninsula are likely recording recent ice-sheet loading history rather than  
154 GIA following the last deglaciation. In particular, a late-Holocene increase in the rate of sea-level  
155 fall could reflect recent ice retreat following a readvance after the last deglaciation, similar to  
156 observations to the south of the West Antarctic ice sheet (Bradley et al., 2015; Kingslake et al.,  
157 2018). This means that relative sea-level data along the Antarctic Peninsula may not be helpful  
158 in constraining last glacial maximum ice volume (Simms et al., 2019), due to the non-monotonic  
159 loading history and the low mantle viscosity of the region resulting in a greater sensitivity to  
160 relatively recent (past few ka) loading changes. Barnett et al. (2018) document both secular and  
161 residual trends in sea-level rise in eastern Quebec. They note a potential glacier mass loss signal  
162 following the Little Ice Age along with influences from the North Atlantic Oscillation, Northern  
163 Hemisphere temperatures and Atlantic meridional overturning circulation. Their results highlight  
164 the complexity in isolating different drivers and thus estimating global mean sea-level change  
165 from local relative sea-level change (e.g., Kopp et al., 2016). Both Simms et al. (2018) and Barnett  
166 et al. (2018) show the difficulty in defining a baseline period in sea level against which current  
167 changes can be assessed and future predictions made.

## 168 **5. Outlook**

169 The papers in this *Quaternary Science Reviews* special issue suggest important avenues for  
170 future research. For the late Pliocene, documenting the magnitude of relative sea-level change in  
171 New Zealand, once corrected for GIA and other tectonic land motions, would provide critical  
172 information on the glacial-interglacial scale of ice-volume change under greenhouse gas  
173 concentrations similar to present. Comparing this independently dated record of sea level to  
174 individual ice-sheet records (e.g., Jansen et al., 2000; Patterson et al., 2014; Blake-Mizen et al.,

175 2019) could test the hypothesis of Raymo et al. (2006) on the lack of precession in the benthic  
176  $\delta^{18}\text{O}$  stack (Fig. 2b) during the late Pliocene to early Pleistocene, which could also help in  
177 understanding the dynamics that led to bipolar Quaternary glaciations.

178 For the last glacial cycle, sea-level budgets are still incomplete. The extent of ice sheets during  
179 MIS 3 (as well as MIS 4 and 5a-d) requires further investigation as does the underlying causes of  
180 the differing ice-sheet extents (e.g., Larsen et al., 2018). Solving the last glacial maximum sea-  
181 level budget should be a critical point of study as over 55 years of research on this topic has not  
182 resulted in closure. This budget problem persists into the deglaciation and the Holocene. At  
183 present, the early Holocene sea-level budget calls for more ice in Antarctica than most  
184 reconstructions have at the last glacial maximum (Cuzzone et al., 2016). Likewise, the sources of  
185 sea-level rise after  $\sim 7$  ka when the Laurentide ice sheet is deglaciated (Ullman et al., 2016) have  
186 to be rectified against the recent observations presented in this special issue. The Greenland ice  
187 sheet was smaller than present and regrew by a modest volume over the late Holocene (e.g.,  
188 Larsen et al., 2015). Similarly, there is growing evidence that the West Antarctic ice sheet was  
189 also smaller than present during the Holocene, regrowing in the late Holocene (Bradley et al.,  
190 2015; Kingslake et al., 2018) as did most glaciers and ice caps in the Northern Hemisphere (e.g.,  
191 Solomina et al., 2015). How these cryospheric changes translate into reconstructions of late-  
192 Holocene global mean sea level changes (e.g., Kopp et al., 2016) should be investigated.

193 Lastly, whether one or more global mean sea-level oscillations occurred during the last  
194 interglaciation should be resolved. Here, the timing and magnitude of individual ice-sheet retreat  
195 histories may also provide important insight. For instance, the Greenland ice sheet retreated  
196 across the last interglaciation, reaching a minimum near the end of the interglacial period (Carlson  
197 et al., 2008b). While no direct evidence exists at present, the Antarctic ice sheets may have been  
198 smaller than present early in the last interglaciation (Dutton et al., 2015b), which can be simulated  
199 by ice-sheet models (e.g., DeConto & Pollard, 2016; Edwards et al., 2019). A global mean sea-



200 level fall and rise could reflect the competing histories of these two ice sheets, with Antarctica  
201 losing mass then regrowing while Greenland continued to retreat through the interglaciation,  
202 rather than retreat and readvance of one ice sheet (Carlson, 2013).

### 203 **Acknowledgements**

204 PALeo constraints on SEA level rise 2 is a Past Global Changes working group and  
205 International Union for Quaternary Research international focus group.

### 206 **References**

207 Alley, R.B., Clark, P.U., Huybrechts, P., Joughin, I., 2005. Ice-sheet and sea-level changes.  
208 *Science* 310, 456-460.

209 Barlow, N.L.M., McClymont, E.L., Whitehouse, P.L., Stokes, C.R., Jamieson, S.S.R., Woodroffe,  
210 S.A., Bentley, M.J., Callard, S.L., Ó Cofaigh, C., Evans, D.J.A., Horrocks, J.R., Lloyd, J.M.,  
211 Long, A.J., Margold, M., Roberts, D.H., Sanchez-Montes, M.L., 2018. Lack of evidence for a  
212 substantial sea-level fluctuation within the Last Interglacial. *Nat. Geosci.*, doi:  
213 10.1038/s41561-018-0195-4.

214 Barnett, R.L., Bernatchez, P., Garneau, M., Brain, M.J., Charman, D.J., Stephenson, D.B., Haley,  
215 S., Sanderson, N., 2019. Late Holocene sea-level changes in eastern Québec and potential  
216 drivers. *Quat. Sci. Rev.* 203, 151-169.

217 Bartoli, G., Hönisch, B., Zeebe, R.E., 2011. Atmospheric CO<sub>2</sub> decline during the Pliocene  
218 intensification of Northern Hemisphere glaciations. *Paleoceanography* 26, doi:  
219 10.1029/2010PA002055.

220 Bereiter, B., Eggleston, S., Schmitt, J., Nehrbass-Ahles, C., Stocker, T.F., Fischer, H., Kipfstuhl,  
221 S., Chappellaz, J., 2015. Revision of the EPICA Dome C CO<sub>2</sub> record from 800 to 600 kyr  
222 before present. *Geophys. Res. Lett.* 42, doi: 10.1002/2014GL061957.

223 Blake-Mizen, K., Hatfield, R.G., Stoner, J.S., Carlson, A.E., Xuan, C., Walczak, M., Lawrence,  
224 K.T., Channell, J.E.T., Bailey, I., 2019. Southern Greenland glaciation and Western Boundary

225 Undercurrent evolution recorded on Eirik Drift during the late Pliocene intensification of  
226 Northern Hemisphere glaciation. *Quat. Sci. Rev.* 209, 40-51.

227 Bradley, S.L., Hindmarsh, R.C.A., Whitehouse, P.L., Bentley, M.J., King, M.A., 2015. Low post-  
228 glacial rebound rates in the Weddell Sea due to Late Holocene ice-sheet readvance. *Earth*  
229 *Planet. Sci. Lett.* 413, 79-89.

230 Carlson, A.E., 2013. Does sea-level volatility indicate individual ice-sheet volatility during the last  
231 interglaciation? PALSEA2 Meeting Abstract, Rome, Italy.

232 Carlson, A.E., LeGrande A.N., Oppo, D.W., Came, R.E., Schmidt, G.A., Anslow, F.S., Licciardi,  
233 J.M., Obbink, E.A., 2008a. Rapid early Holocene deglaciation of the Laurentide Ice Sheet.  
234 *Nat. Geosci.* 1, 620-624.

235 Carlson, A.E., Stoner, J.S., Donnelly, J.P., Hillaire-Marcel, C., 2008b. Response of the southern  
236 Greenland Ice Sheet during the last two deglaciations. *Geology* 36, 359-362.

237 Carlson, A.E., Tarasov, L., Pico, T., 2018. Rapid Laurentide ice-sheet advance towards southern  
238 last glacial maximum limit during marine isotope stage 3. *Quat. Sci. Rev.* 196, 118-123.

239 Ceperley, E., Marcott, S., Rawling III, J.E., Zoet, L., Zimmerman, S., 2019. The role of permafrost  
240 on the morphology of an MIS 3 moraine from the southern Laurentide Ice Sheet. *Geology* in  
241 press.

242 Church, J.A., Clark, P.U., Cazenave, A., Gregory, J.M., Jevrejeva, S., Levermann, A., Merrifield,  
243 M.A., Milne, G.A., Nerem, R.S., Nunn, P.D. Payne, A.J., Pfeffer, W.T., Stammer, D.,  
244 Unnikrishnan, A.S., 2013. *Sea Level Change*. Cambridge University Press, Cambridge,  
245 United Kingdom and New York, NY, USA.

246 Clark, P.U., Mix, A.C., 2002. Ice sheets and sea level at the Last Glacial Maximum. *Quat. Sci.*  
247 *Rev.* 21, 1-7.

248 Clark, P.U., Tarasov, L., 2014. Closing the sea level budget at the Last Glacial Maximum.  
249 *Proceed. Nat. Acad. Sci.* 111, 15861-15862.

250 Clark, P.U., Clague, J.J., Curry, B.B., Dreimanis, A., Hicock, S.R., Miller, G.H., Berger, G.W.,  
251 Eyles, N., Lamothe, M., Miller, B.B., Mott, R.J., Oldale, R.N., Stea, R.R., Szabo, J.P.,  
252 Thorleifson, L.H., Vincent, J.-S., 1993. Initiation and development of the Laurentide and  
253 Cordilleran ice sheets following the last interglaciation. *Quat. Sci. Rev.* 12, 79-114.

254 Clark, P.U., Dyke, A.S., Shakun, J.D., Carlson, A.E., Clark, J., Wohlfarth, B., Hostetler, S.W.,  
255 Mitrovica, J.X., McCabe, A.M., 2009. The Last Glacial Maximum. *Science* 325, 710-714.

256 Clark, P.U., Shakun, J.D., Marcott, S.A., Mix, A.C., Eby, M., Kulp, S., Levermann, A., Milne, G.A.,  
257 Pfister, P.L., Santer, B.D., Schrag, D.P., Solomon, S., Stocker, T.F., Strauss, B.H., Weaver,  
258 A.J., Winkelmann, R., Archer, D., Bard, E., Goldner, A., Lambeck, K., Pierrehumbert, R.T.,  
259 Plattner, G.-K., 2016. Consequences of twenty-first-century policy for multi-millennial climate  
260 and sea-level change. *Nat. Clim. Change*, doi: 10.1038/NCLIMATE2923.

261 Cuzzone, J.K., Clark, P.U., Carlson, A.E., Ullman, D.J., Rinterknecht, V.R., Milne, G.A., Pekka,  
262 J., Wohlfarth, B., Marcott, S.A., Caffee, M., 2016. Final deglaciation of the Scandinavian Ice  
263 Sheet and implications for the Holocene global sea-level budget. *Earth Planet. Sci. Lett.* 448,  
264 34-41.

265 Dalton, A.S., Finkelstein, S.A., Barnett, P.J., Forman, S.L., 2016. Constraining the late  
266 Pleistocene history of the Laurentide ice sheet by dating the Missinaibi formation, Hudson Bay  
267 lowlands, Canada. *Quat. Sci. Rev.* 146, 288-299.

268 Dalton, A.S., Finkelstein, S.A., Forman, S.L., Barnett, P.J., Pico, T., Mitrovica, J.X., 2019. Was  
269 the Laurentide Ice Sheet significantly reduced during Marine Isotope Stage 3? *Geology*, doi:  
270 10.1130/G45335.1.

271 Darvill, C.M., Menounos, B., Goehring, B.M., Lian, O.B., Caffee, M.W., 2018. Retreat of the  
272 western Cordilleran Ice Sheet margin during the last deglaciation. *Geophys. Res. Lett.* 45,  
273 doi: 10.1029/2018GL079419.

274 DeConto, R.M., Pollard, D., 2016. Contribution of Antarctica to past and future sea-level rise.  
275 Nature 531, 591-597.

276 Denton, G.H., Hughes, T.J., 1981. The Last Great Ice Sheets, Wiley, New York, 484pp.

277 Denton, G.H., Anderson, R.F., Toggweiler, J.R., Edwards, R.L., Schaefer, J.M., Putnam, A.E.,  
278 2010. The last glacial termination. Science 328, 1652-1656.

279 Donn, W.L., Farrand, W.R., Ewing, M., 1962. Pleistocene ice volumes and sea-level lowering. J.  
280 Geol. 70, 206-214.

281 Dutton, A., Carlson, A.E., Long, A.J., Milne, G.A., Clark, P.U., DeConto, R., Horton, B., Rahmstorf,  
282 S., Raymo, M.E., 2015a. Sea-level rise due to polar ice-sheet mass loss during past warm  
283 periods. Science 349, 153.

284 Dutton, A., Webster, J.M., Zwartz, D., Lambeck, K., Wohlfarth, B., 2015b. Tropical tales of polar  
285 ice: evidence of Last Interglacial polar ice sheet retreat recorded by fossil reefs of the granitic  
286 Seychelles islands. Quat. Sci. Rev. 107, 182-196.

287 Edwards, T.L., Brandon, M.A., Durand, G., Edwards, N.R., Golledge, N.R., Holden, P.B., Nias,  
288 I.J., Payne, A.J., Ritz, C., Wernecke, A., 2019. Revisiting Antarctic ice loss due to marine ice-  
289 cliff instability. Nature 566, 58-64.

290 Grant, G.R., Sefton, J.P., Patterson, M.W., Naish, T.R., Dunbar, G.B., Hayward, B.W., Morgans,  
291 H.E.G., Alloway, B.V., Seward, D., Tapai, C.A., Prebble, J.G., Kamp, P.J.J, McKay, R.,  
292 Ohneiser, C., Turner, G.M., 2018. Mid- to late Pliocene (3.3-2.6 Ma) global sea-level  
293 fluctuations recorded on a continental shelf transect, Whanganui Basin, New Zealand. Quat.  
294 Sci. Rev. 201, 241-260.

295 Hallmann, N., Camoin, G., Eisenhauer, A., Botella, A., Milne, G.A., Vella, C., Samankassou, E.,  
296 Pothin, V., Dussouillez, P., Fleury, J., Fietzke, J., 2018. Ice volume and climate changes from  
297 a 6000 year sea-level record in French Polynesia. Nat. Comm., doi: 10.1038/s41467-017-  
298 02695-7.

299 Jansen, E., Fronval, T., Rack, F., Channell, J.E.T., 2000. Pliocene-Pleistocene ice rafting history  
300 and cyclicity in the Nordic Seas during the last 3.5 Myr. *Paleoceanography* 15, 709-721.

301 Kingslake, J., Scherer, R.P., Albrecht, T., Coenen, J., Powell, R.D., Reese, R., Stansell, N.D.,  
302 Tulaczyk, S., Wearing, M.G., Whitehouse, P.L., 2018. Extensive retreat and re-advance of the  
303 West Antarctic Ice Sheet during the Holocene. *Nature* 558, 430-434.

304 Kopp, R.E., Kemp, A.C., Bittermann, K., Horton, B.P., Donnelly, J.P., Gehrels, W.R., Hay, C.C.,  
305 Mitrovica, J.X., Morrow, E.D., Rahmstorf, S., 2016. Temperature-driven global sea-level  
306 variability in the Common Era. *Proceed. Nat. Acad. Sci.*, doi: 10.1073/pnas.1517056113.

307 Kopp, R.E., Simons, F.J., Mitrovica, J.X., Maloof, A.C., Oppenheimer, M., 2013. A probabilistic  
308 assessment of sea level variations within the last interglacial stage. *Geophys. J. Int.*, doi:  
309 10.1093/gji/ggt029.

310 Lambeck, K., Rouby, H., Purcell, A., Sun, Y., Sambridge, M., 2014. Sea level and global ice  
311 volumes from the last glacial maximum to the Holocene. *Proc. Natl. Acad. Sci.*, doi:  
312 10.1073/pnas.1411762111.

313 Larsen, N.K., Kjær, K.H., Lecavalier, B., Bjørk, A.A., Colding, S., Huybrechts, P., Jakobsen, K.E.,  
314 Kjeldsen, K.K., Knudsen, K.-L., Odgaard, B.V., Olsen, J., 2015. The response of the southern  
315 Greenland ice sheet to the Holocene thermal maximum. *Geology*, doi: 10.1130/G36476.1.

316 Larsen, N.K., Levy, L.B., Carlson, A.E., Buizert, C., Olsen, J., Strunk, A., Bjørk, A.A., Skov, D.S.,  
317 2018. Instability of the Northeast Greenland Ice Stream over the last 45,000 years. *Nat.*  
318 *Commun.*, doi: 10.1038/s41467-018-04312-7.

319 Laskar, J., Robutel, P., Joutel, F., Gastineau, M., Correia, A.C.M., Levrard, B., 2004. A long-term  
320 numerical solution for the insolation quantities of the Earth. *Astronomy & Astrophysics* 428,  
321 261-285.

322 Lesnek, A.J., Briner, J.P., Lindqvist, C., Baichtal, J.F., Heaton, T.H., 2018. Deglaciation of the  
323 Pacific coastal corridor directly preceded the human colonization of the Americas. *Sci. Adv.*  
324 4, eaar5040.

325 Lisiecki, L.E., Raymo, M.E., 2005. A Pliocene-Pleistocene stack of 57 globally distributed benthic  
326  $\delta^{18}\text{O}$  records. *Paleoceanography* 20, doi: 10.1029/2004PA001071.

327 Martínez-Botí, M.A., Foster, G.L., Chalk, T.B., Rohling, E.J., Sexton, P.F., Lunt, D.J., Pancost,  
328 R.D., Badger, M.P.S., Schmidt, D.N., 2015. Plio-Pleistocene climate sensitivity evaluated  
329 using high-resolution  $\text{CO}_2$  records. *Nature* 518, 49-54.

330 Meyers, S.R., Hinnov, L.A., 2010. Northern Hemisphere glaciation and the evolution of Plio-  
331 Pleistocene climate noise. *Paleoceanography* 25, doi: 10.1029/2009PA001834.

332 Mix, A.C., Pisias, N.G., Rugh, W., Wilson, J., Morey, A., Hagelberg, T.K., 1995. Benthic  
333 foraminifer stable isotope record from Site 849 (0–5 Ma): local and global climate changes.  
334 *Proc. ODP, Sci. Results* 138, 371–412.

335 Patterson, M.O., McKay, R., Naish, T., Escutia, C., Jimenez-Epejo, F.J., Raymo, M.E., Meyers,  
336 S.R., Tauxe, L., Brinkhuis, H., IODP Expedition 318 Scientists, 2014. Orbital forcing of the  
337 East Antarctic ice sheet during the Pliocene and early Pleistocene. *Nat. Geosci.*, doi:  
338 10.1038/NGEO2273.

339 Pearson, P.N., Palmer, M.R., 2000. Atmospheric carbon dioxide concentrations over the past 60  
340 million years. *Nature* 406, 695-699.

341 Peltier, W.R., Fairbanks, R.G., 2006. Global glacial ice volume and Last Glacial Maximum  
342 duration from an extended Barbados sea level record. *Quat. Sci. Rev.* 25, 3322-3337.

343 Pico, T., Birch, L., Weisenberg, J., Mitrovica, J.X., 2018. Refining the Laurentide Ice Sheet at  
344 Marine Isotope Stage 3: A data-based approach combining glacial isostatic simulations with  
345 a dynamic ice model. *Quat. Sci. Rev.* 195, 171-179.

346 Pico, T., Creveling, J.R., Mitrovica, J.X., 2017. Sea-level records from the U.S. Mid-Atlantic  
347 constrain Laurentide ice sheet extent during marine isotope stage 3. *Nat. Commun.*, doi:  
348 10.1038/ncomms15612.

349 Polyak, V.J., Onac, B.P./., Fornós, J.J., Hay, C., Asmerom, Y., Dorale, J.A., Ginés, J., Tuccimei,  
350 P., Ginés, A., 2018. A highly resolved record of relative sea level in the western Mediterranean  
351 Sea during the last interglacial period. *Nat. Geosci.*, doi: 10.1038/s41561-018-0222-5.

352 Raymo, M.E., Lisiecki, L.E., Nisancioglu, K.H., 2006. Plio-Pleistocene ice volume, Antarctic  
353 climate, and the global  $\delta^{18}\text{O}$  record. *Science* 313, 492-495.

354 Romundset, A., Lakeman, T.R., Høgaas, F., 2018. Quantifying variable rates of postglacial  
355 relative sea level fall from a cluster of 24 isolation basins in southern Norway. *Quat. Sci. Rev.*  
356 197, 175-192.

357 Simms, A.R., Lisiecki, L., Gebbie, G., Whitehouse, P.L., Clark, J.F., 2019. Balancing the last  
358 glacial maximum (LGM) sea-level budget. *Quat. Sci. Rev.* 205, 143-153.

359 Simms, A.R., Whitehouse, P.L., Simkins, L.M., Nield, G., DeWitt, R., Bentely, M.J., 2018. Late  
360 Holocene relative sea levels near Palmer Station, northern Antarctic Peninsula, strongly  
361 controlled by late Holocene ice-mass changes. *Quat. Sci. Rev.* 199, 49-59.

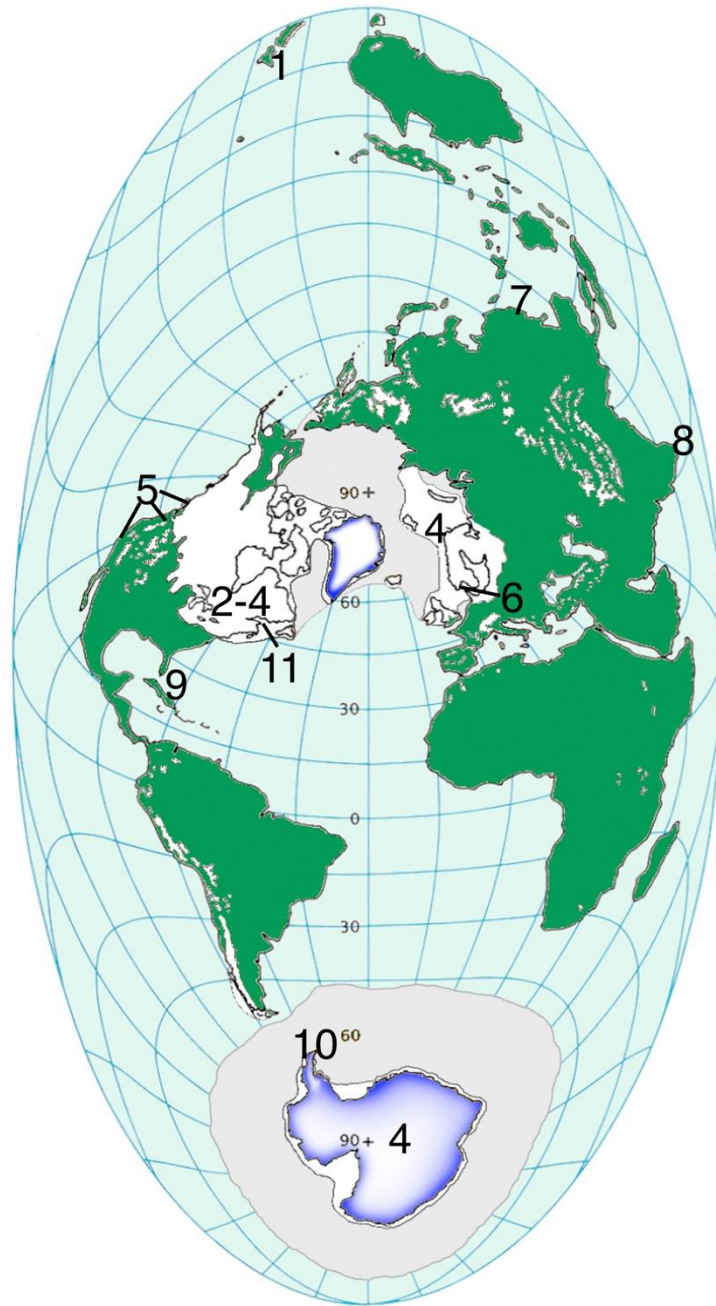
362 Skrivanek, A., Li, J., Dutton, A.E., 2018. Relative sea-level change during the Last Interglacial as  
363 recorded in Bahamian fossil reefs. *Quat. Sci. Rev.* 200, 160-177.

364 Solomina, O.N., Bradley, R.S., Hodgson, D.A., Ivy-Ochs, S., Jomelli, V., Mackintosh, A.N., Nesje,  
365 A., Owen, L.A., Wanner, H., Wiles, G.C., Young, N.E., 2015. Holocene glacier fluctuations.  
366 *Quat. Sci. Rev.* 111, 9-34.

367 Thompson, W.G., Curran, H.A., Wilson, M.A., White, B., 2011. Sea-level oscillations during the  
368 last interglacial highstand recorded by Bahamas corals. *Nat. Geosci.*, doi:  
369 10.1038/NGEO1253.

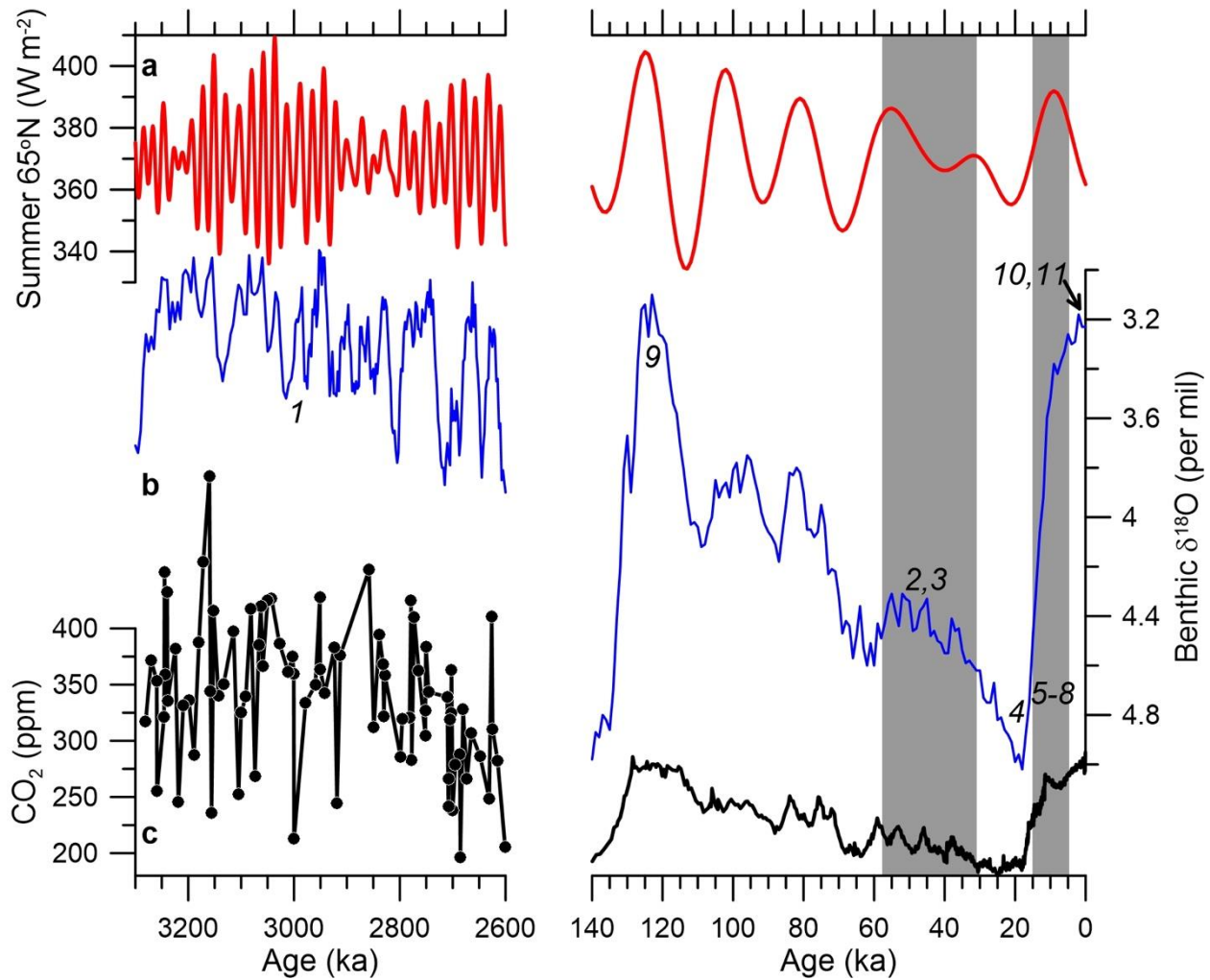
- 370 Ullman, D.J., Carlson, A.E., Hostetler, S.W., Clark, P.U., Cuzzone, J.K., Milne, G.A., Winsor, K.,  
371 Caffee, M., 2016. Final deglaciation of the Laurentide ice sheet in the early to middle  
372 Holocene. *Quat. Sci. Rev.* 152, 49-59.
- 373 Wood, J.R., Forman, S.L., Everton, D., Pierson, J., Gomez, J., 2010. Lacustrine sediments in  
374 Porter Cave, Central Indiana, USA and possible relation to Laurentide ice sheet marginal  
375 positions in the middle and late Wisconsinan. *Palaeogeog., Palaeoclim., Palaeoecol.* 298,  
376 421-431.
- 377 Xiong, H., Zong, Y., Qian, P., Huang, G., Fu, S., 2018. Holocene sea-level history of the northern  
378 coast of South China Sea. *Quat. Sci. Rev.* 194, 12-26.
- 379 Yokoyama, Y., Hirabayashi, S., Goto, K., Okuno, J., Sproson, A.D., Haraguchi, T., Ratnayake,  
380 N., Miyairi, Y., 2019. Holocene Indian Ocean sea level, Antarctic melting history and past  
381 Tsunami deposits inferred using sea level reconstructions from the Sri Lankan, Southeastern  
382 Indian and Maldivian coasts. *Quat. Sci. Rev.* 206, 150-161.
- 383 Yousefi, M., Milne, G.A., Love, R., Tarasov, L., 2018. Glacial isostatic adjustment along the Pacific  
384 coast of central North America. *Quat. Sci. Rev.* 193, 288-311.





385

386 **Fig. 1.** Map of ice-sheet extent at the last glacial maximum (Denton et al., 2010). Numbers indicate  
 387 the location of studies in this special issue: 1 – Grant et al. (2018); 2 – Carlson et al. (2018); 3 –  
 388 Pico et al. (2018); 4 – Simms et al. (2019a); 5 – Yousefi et al. (2018); 6 – Romundset et al. (2018);  
 389 7 – Xiong et al. (2018); 8 – Yokoyama et al. (2019); 9 – Skrivanek et al. (2018); 10 – Simms et al.  
 390 (2018b); 11 – Barnett et al. (2019).



391

392 **Fig. 2.** Time series for the late Pliocene (left) and the last glacial cycle (right). (a) Summer

393 (average of summer solstice to fall equinox) insolation at 65°N (Laskar et al., 2004). (b) benthic

394  $\delta^{18}\text{O}$  (Lisiecki & Raymo, 2005). Italics numbers (see Fig. 1) indicate the time periods covered by

395 individual studies in this special issue, with gray bars denoting the range of study during marine

396 isotope stage 3 and the early to middle Holocene. (c) Atmospheric  $\text{CO}_2$  concentration from

397 planktic foraminifer  $\delta^{11}\text{B}$  (left with symbols; Pearson & Palmer, 2000; Bartoli et al., 2011; Martínez-

398 Botí et al., 2015) and ice-core measurements (right with thick line; Bereiter et al., 2015).